Mathematical Problems in Engineering, 2002, Vol. 8(6), pp. 517–539 Taylor & Francis
Taylor & Francis Group

Eigenstructure of the Equilateral Triangle, Part II: The Neumann Problem

BRIAN J. McCARTIN*

Applied Mathematics, Kettering University, 1700 West Third Avenue, Flint, Michigan, 48504-4898

Dedicated to Professor Ghasi Verma for passing on the Art of Applied Mathematics.

Lamé's formulas for the eigenvalues and eigenfunctions of the Laplacian with Neumann boundary conditions on an equilateral triangle are derived using direct elementary mathematical techniques. They are shown to form a complete orthonormal system. Various properties of the spectrum and nodal lines are explored. Implications for related geometries are considered.

Key words: Equilateral triangle; Laplacian eigenvalues/eigenvectors; Neumann problem

AMS subject classifications: 35C05, 35J05, 35P10

1 INTRODUCTION

It is well known that the collection of two dimensional domains for which the eigenstructure of the Laplacian is available explicitly contains rectangles and ellipses. It is not nearly so widely recognized that the equilateral triangle also belongs to this class of regions. The eigenvalues and eigenfunctions of the Laplacian on an equilateral triangle were first presented by Lamé [4–6] and then further explored by Pockels [11].

However, Lamé did not provide a complete derivation of his formulas but rather simply stated them and then showed that they satisfied the relevant equation and associated boundary conditions. Most subsequent authors have either simply made reference to the work of Lamé [13] or reproduced his formulas without derivation [11, 15]. One notable exception is the work of Pinsky [10] where Lamé's formulas are derived using the functional analytic technique of reflection operators due to Arnold. Another is the more recent work of Práger [12] wherein these eigenfunctions are derived via an indirect procedure based upon prolongation/folding transformations relating the equilateral triangle and an associated rectangle. Thus, there is presently a lacuna in the applied mathematical literature as concerns a direct elementary treatment of the eigenstructure of the equilateral triangle.

It is the express purpose of the present work to fill this gap for the case of the Neumann boundary condition. The parallel development for the Dirichlet problem appears in [8]. A forthcoming part will present a corresponding treatment of the Robin problem. Not only will we supply a derivation of Lamé's formulas from first principles but we will also endeavor to provide an extensive account of modal properties. Many of these properties are simply stated

* E-mail: bmccarti@kettering.edu

ISSN 1024-123X print; ISSN 1563-5147 online

by Lamé and Pockels but herein receive full derivation. Other properties that are clearly identified below are new and appear here for the first time.

Knowing the eigenstructure permits us to construct the Neumann function, and we do so. The implications for related geometries are also explored. The primarily pedagogical and historical exposition to follow gladly trades off mathematical elegance for brute-force, yet straightforward, computation in the hope that these interesting results will thereby find their natural place in introductory treatments of boundary value problems.

2 THE NEUMANN EIGENPROBLEM FOR THE EQUILATERAL TRIANGLE

During his investigations into the cooling of a right prism with equilateral triangular base [5], Lamé was led to consider the eigenvalue problem

$$\Delta T(x,y) + k^2 T(x,y) = 0, \quad (x,y) \in \tau; \qquad \frac{\partial T}{\partial \nu}(x,y) = 0, \quad (x,y) \in \partial\tau \tag{2.1}$$

where Δ is the two-dimensional Laplacian, $\partial^2/\partial x^2 + \partial^2/\partial y^2$, τ is the equilateral triangle shown in Figure 2.1, and ν its outward pointing normal. Remarkably, he was able to show that the eigenfunctions satisfying Eq. (2.1) could be expressed in terms of combinations of sines and cosines, typically the province of rectangular geometries [7].

Lamé later encountered the same eigenproblem when considering the vibrational modes of a free elastic membrane in the shape of an equilateral triangle [6]. The identical problem occurs also in acoustic ducts with hard walls and in the propagation of transverse electric (TE- or H-) modes in electromagnetic waveguides [3]. Lamé's solution of this problem actually proceeds from quite general considerations about precisely which geometries will give rise to eigenfunctions composed of sines and cosines. These matters we now take up.

3 LAMÉ'S FUNDAMENTAL THEOREM

Let us begin by stating that we will make some alterations to Lamé's presentation of his General Law of a Nodal Plane. First of all, rather than being concerned with three-dimensional problems, we will restrict attention to two dimensions and hence will consider instead nodal lines (*i.e.*, lines along which an eigenfunction vanishes) and antinodal lines (along which the normal derivative vanishes). Secondly, since we are not specifically interested in

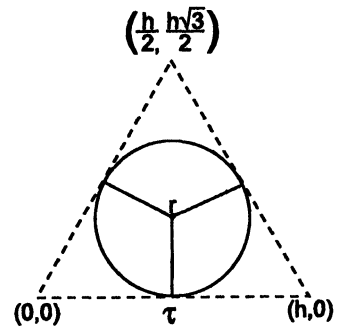

FIGURE 2.1 Equilateral triangle with incircle.

heat transfer but rather in the eigenproblem, Eq. (2.1), in its own right, we will replace his notions of inverse/direct calorific symmetry by the less application-specific concepts of antisymmetry/symmetry, respectively.

Motivated by his earlier work in crystallography, Lamé made the following observations the cornerstone of his work on heat transfer in right prisms (see [8] for a complete elementary proof).

THEOREM 3.1 (Fundamental Theorem) *Suppose that $T(x,y)$ can be represented by the trigonometric series*

$$T(x,y) = \sum_i A_i \sin(\lambda_i x + \mu_i y + \alpha_i) + B_i \cos(\lambda_i x + \mu_i y + \beta_i) \tag{3.1}$$

with $\lambda_i^2 + \mu_i^2 = k^2$, then

(i) *$T(x,y)$ is antisymmetric about any line along which it vanishes.*
(ii) *$T(x,y)$ is symmetric about any line along which its normal derivative, $\partial T/\partial \nu$, vanishes.*

The Fundamental Theorem has the following immediate consequences.

COROLLARY 3.2 *With $T(x,y)$ as defined by Eq.* (3.1),

(i) *If $T = 0$ along the boundary of a polygon then $T = 0$ along the boundaries of the family of congruent and symmetrically placed polygons obtained by reflection about its sides.*
(ii) *if $\partial T/\partial \nu = 0$ along the boundary of a polygon then $\partial T/\partial \nu = 0$ along the boundaries of the family of congruent and symmetrically placed polygons obtained by reflection about its sides.*

This corollary has far reaching implications for the determination of those domains which possess eigenfunctions expressible in terms of sines and cosines (henceforth referred to as "trigonometric eigenfunctions"). For example, Figure 3.1 illustrates that the diagonal of a rectangle cannot ordinarily be a nodal line, nor for that matter an antinodal line, since the rectangle has a complete orthonormal system of trigonometric eigenfunctions yet does not possess the requisite symmetry unless it is either a square or has aspect ratio $\sqrt{3}$ (see Fig. 8.7). Here and below, solid lines denote lines of asymmetry while dashed lines denote lines of symmetry. Furthermore, as illustrated in Figure 3.2, a right isosceles triangle may be repeatedly reflected about its edges to produce the symmetry (denoted by +) required by the Fundamental Theorem and in fact possesses trigonometric eigenfunctions obtained from the restriction of those of a square with an antinodal line along a fixed diagonal.

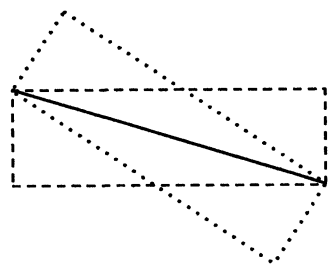

FIGURE 3.1 Rectangular reflection.

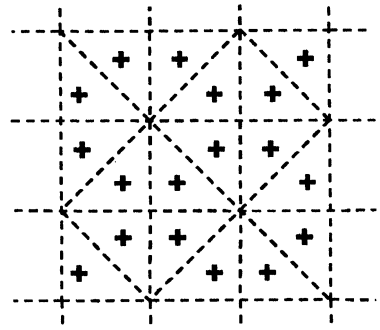

FIGURE 3.2 Symmetry of isosceles right triangle.

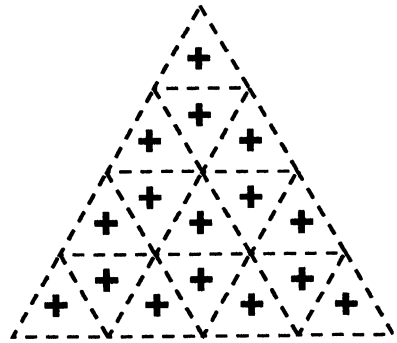

FIGURE 3.3 Symmetry of equilateral triangular lattice.

Next consider the equilateral triangular lattice of Figure 3.3 together with its supporting symmetric structure. It suggests that the equilateral triangle *might* possess trigonometric eigenfunctions since the Fundamental Theorem supplies necessary but not sufficient conditions. By devices unknown, Lamé was in fact able to construct such a family of eigenfunctions but, before we can even describe them, we must first introduce his natural triangular coordinate system. We will return to consider other regions with and without trigonometric eigenfunctions in a later section.

4 TRIANGULAR COORDINATE SYSTEM

Reconsider the equilateral triangle of side h in standard position in Cartesian coordinates (x, y) (Fig. 2.1) and define the **triangular coordinates** (u, v, w) of a point P (Fig. 4.1) by

$$\begin{aligned} u &= r - y \\ v &= \frac{\sqrt{3}}{2}\left(x - \frac{h}{2}\right) + \frac{1}{2}(y - r) \\ w &= \frac{\sqrt{3}}{2}\left(\frac{h}{2} - x\right) + \frac{1}{2}(y - r) \end{aligned} \tag{4.1}$$

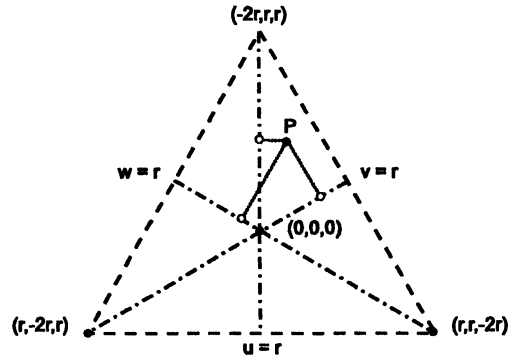

FIGURE 4.1 Triangular coordinate system.

where $r = h/(2\sqrt{3})$ is the inradius of the triangle. The coordinates u, v, w may be described as the distances of the triangle center to the projections of the point onto the altitudes, measured positively toward a side and negatively toward a vertex.

Note that the triangular coordinates satisfy the relation

$$u + v + w = 0. \tag{4.2}$$

Moreover, the center of the triangle has coordinates (0, 0, 0) and the three sides of the triangle are given by $u = r$, $v = r$, and $w = r$, thus simplifying the application of boundary conditions. They are closely related to the barycentric coordinates (U, V, W) introduced by his contemporary Möbius in 1827 [2]:

$$\begin{aligned} U &= \frac{r-u}{3r} \\ V &= \frac{r-v}{3r} \\ W &= \frac{r-w}{3r} \end{aligned} \tag{4.3}$$

satisfying $U + V + W = 1$. These were destined to become the darling of finite element practitioners in the 20th Century.

5 SEPARATION OF VARIABLES

We now commence with our original, complete, direct, and elementary derivation by introducing the orthogonal coordinates (ξ, η) given by

$$\xi = u, \qquad \eta = v - w, \tag{5.1}$$

Equation (2.1) becomes

$$\frac{\partial^2 T}{\partial \xi^2} + 3\frac{\partial^2 T}{\partial \eta^2} + k^2 T = 0. \tag{5.2}$$

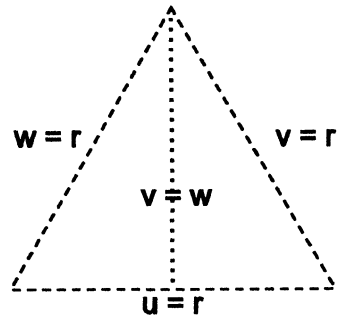

FIGURE 5.1 Modal line of symmetry/antisymmetry.

Hence, if we seek a separated solution of the form

$$f(\xi) \cdot g(\eta) \tag{5.3}$$

we arrive at

$$f'' + \alpha^2 f = 0; \qquad g'' + \beta^2 g = 0; \qquad \alpha^2 + 3\beta^2 = k^2. \tag{5.4}$$

Thus, there exist separated solutions of the form

$$f(u) \cdot g(v - w), \tag{5.5}$$

where f and g are trigonometric functions.

Before proceeding any further, we will decompose the sought after eigenfunction into parts symmetric and antisymmetric about the altitude $v = w$ (see Fig. 5.1)

$$T(u, v, w) = T_s(u, v, w) + T_a(u, v, w), \tag{5.6}$$

where

$$T_s(u, v, w) = \frac{T(u, v, w) + T(u, w, v)}{2}; \; T_a(u, v, w) = \frac{T(u, v, w) - T(u, w, v)}{2}, \tag{5.7}$$

henceforth to be dubbed a symmetric/antisymmetric mode, respectively. We next take up the determination of T_s and T_a separately.

6 CONSTRUCTION OF A SYMMETRIC MODE

We first dispense with the eigenvalue $k^2 = 0$. Its corresponding eigenvector is constant and we choose $T_s^{0,0} = 3$ for reasons that will become evident. There is no corresponding antisymmetric mode. Any multiple of this symmetric mode, shown in Figure 6.1, is called a plane wave. We next search for symmetric modes which are not plane waves.

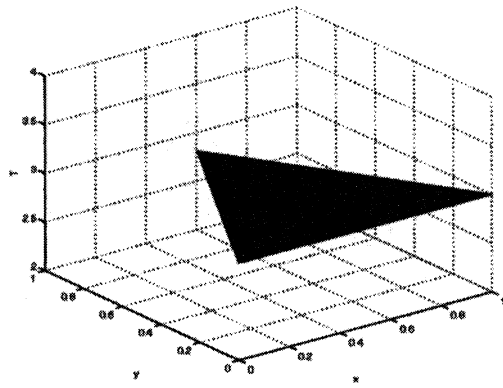

FIGURE 6.1 Plane wave.

In light of the fact that $\partial T_s/\partial u$ must vanish when $u = -2r$ and $u = r$ while being even as a function of $v - w$, we seek a solution of the form

$$T_s = \cos\left[\frac{\pi l}{3r}(u + 2r)\right] \cos[\beta_1(v - w)], \tag{6.1}$$

where l is an integer and $[\pi l/3r]^2 + 3\beta_1^2 = k^2$. We will show that, by itself, this form cannot satisfy the Neumann boundary condition along $v = r$. Observe that if it could then, by symmetry, it would automatically satisfy the corresponding boundary condition along $w = r$.

Moreover, we will show that the sum of two such terms also does not suffice for the satisfaction of the remaining boundary conditions. However, the sum of three appropriately chosen terms of the form Eq. (6.1) does indeed satisfy said boundary conditions and thus constitutes the sought after symmetric mode. In the course of this demonstration, the expression for the eigenvalues k^2 will emerge.

Along $v = r$, we have $v - w = u + 2r$ where we have invoked the fundamental relation of triangular coordinates given by Eq. (4.2). In order to facilitate the calculation of the normal derivative along $v = r$, we will utilize the coordinate system $(w - u, w + u)$. In terms of these coordinates, $u = -(1/2)(w - u) + (1/2)(w + u)$, $v = -(w + u)$, $w = (1/2)(w - u) + (1/2)(w + u)$, and $v - w = -(1/2)(w - u) - (3/2)(w + u)$ so that

$$\begin{aligned}\frac{\partial T_s}{\partial(w + u)}\Big|_{v=r} = &\left(\frac{3}{4}\beta_1 - \frac{\pi l}{12r}\right) \sin\left[\left(\frac{\pi l}{3r} + \beta_1\right)(u + 2r)\right] \\ &+ \left(\frac{3}{4}\beta_1 + \frac{\pi l}{12r}\right) \sin\left[\left(-\frac{\pi l}{3r} + \beta_1\right)(u + 2r)\right],\end{aligned} \tag{6.2}$$

which cannot be identically equal to zero $-2r \le u \le r$ unless $l = 0$ and $\beta_1 = 0$ in which case Eq. (6.1) degenerates to a plane wave. Thus, one such term does not suffice.

Hence, let us try instead a sum of the form

$$T_s = \cos\left[\frac{\pi l}{3r}(u + 2r)\right] \cos[\beta_1(v - w)] + \cos\left[\frac{\pi m}{3r}(u + 2r)\right] \cos[\beta_2(v - w)], \tag{6.3}$$

with $[\pi l/(3r)]^2 + 3\beta_1^2 = [\pi m/(3r)]^2 + 3\beta_2^2 = k^2$. Along $v = r$, we now have

$$\begin{aligned}\frac{\partial T_s}{\partial(w+u)}\Big|_{v=r} &= \left(\frac{3}{4}\beta_1 - \frac{\pi l}{12r}\right)\sin\left[\left(\frac{\pi l}{3r} + \beta_1\right)(u+2r)\right] \\ &+ \left(\frac{3}{4}\beta_1 + \frac{\pi l}{12r}\right)\sin\left[\left(-\frac{\pi l}{3r} + \beta_1\right)(u+2r)\right] \\ &+ \left(\frac{3}{4}\beta_2 - \frac{\pi m}{12r}\right)\sin\left[\left(\frac{\pi m}{3r} + \beta_2\right)(u+2r)\right] \\ &+ \left(\frac{3}{4}\beta_2 + \frac{\pi m}{12r}\right)\sin\left[\left(-\frac{\pi m}{3r} + \beta_2\right)(u+2r)\right], \end{aligned} \tag{6.4}$$

and the only way to get these terms to cancel pairwise is to choose $l = m = \beta_1 = \beta_2 = 0$ which once again produces only a plane wave. Thus, two such terms do not suffice.

Undaunted, we persevere to consider a sum of the form

$$\begin{aligned} T_s &= \cos\left[\frac{\pi l}{3r}(u+2r)\right]\cos[\beta_1(v-w)] \\ &+ \cos\left[\frac{\pi m}{3r}(u+2r)\right]\cos[\beta_2(v-w)] \\ &+ \cos\left[\frac{\pi n}{3r}(u+2r)\right]\cos[\beta_3(v-w)], \end{aligned} \tag{6.5}$$

with

$$\left[\frac{\pi l}{3r}\right]^2 + 3\beta_1^2 = \left[\frac{\pi m}{3r}\right]^2 + 3\beta_2^2 = \left[\frac{\pi n}{3r}\right]^2 + 3\beta_3^2 = k^2. \tag{6.6}$$

Along $v = r$, we now have

$$\begin{aligned}\frac{\partial T_s}{\partial(w+u)}\Big|_{v=r} &= \left(\frac{3}{4}\beta_1 - \frac{\pi l}{12r}\right)\sin\left[\left(\frac{\pi l}{3r} + \beta_1\right)(u+2r)\right] \\ &+ \left(\frac{3}{4}\beta_1 + \frac{\pi l}{12r}\right)\sin\left[\left(-\frac{\pi l}{3r} + \beta_1\right)(u+2r)\right] \\ &+ \left(\frac{3}{4}\beta_2 - \frac{\pi m}{12r}\right)\sin\left[\left(\frac{\pi m}{3r} + \beta_2\right)(u+2r)\right] \\ &+ \left(\frac{3}{4}\beta_2 + \frac{\pi m}{12r}\right)\sin\left[\left(-\frac{\pi m}{3r} + \beta_2\right)(u+2r)\right] \\ &+ \left(\frac{3}{4}\beta_3 - \frac{\pi n}{12r}\right)\sin\left[\left(\frac{\pi n}{3r} + \beta_3\right)(u+2r)\right] \\ &+ \left(\frac{3}{4}\beta_3 + \frac{\pi n}{12r}\right)\sin\left[\left(-\frac{\pi n}{3r} + \beta_3\right)(u+2r)\right], \end{aligned} \tag{6.7}$$

There are now eight possible ways that cancellation may occur that all lead to essentially the same conclusion. Hence, we pursue in detail only

$$\frac{\pi l}{3r}+\beta_1=-\frac{\pi n}{3r}+\beta_3;\quad \frac{\pi l}{3r}-\beta_1=-\frac{\pi m}{3r}-\beta_2;\quad \frac{\pi m}{3r}-\beta_2=-\frac{\pi n}{3r}-\beta_3. \tag{6.8}$$

When added together, these three equations yield the important relation

$$l+m+n=0. \tag{6.9}$$

With this consistency condition satisfied, we may add the first and last of Eqs. (6.8) to obtain

$$\beta_1-\beta_2=\frac{\pi}{3r}(l+m), \tag{6.10}$$

which, when combined with the identity

$$3(\beta_1-\beta_2)(\beta_1+\beta_2)=\left(\frac{\pi}{3r}\right)^2(m-l)(m+l) \tag{6.11}$$

obtained by rearranging the first of Eqs. (6.6), yields

$$\beta_1+\beta_2=\frac{\pi}{9r}(m-l) \tag{6.12}$$

and, finally,

$$\beta_1=\frac{\pi(m-n)}{9r};\quad \beta_2=\frac{\pi(n-l)}{9r};\ \beta_3=\frac{\pi(l-m)}{9r}. \tag{6.13}$$

The eigenvalue may now be calculated as

$$k^2=\frac{2}{27}\left(\frac{\pi}{r}\right)^2[l^2+m^2+n^2]=\frac{4}{27}\left(\frac{\pi}{r}\right)^2[m^2+mn+n^2], \tag{6.14}$$

with the corresponding symmetric mode given by

$$\begin{aligned}T_s^{m,n}=&\cos\left[\frac{\pi l}{3r}(u+2r)\right]\cos\left[\frac{\pi(m-n)}{9r}(v-w)\right]\\&+\cos\left[\frac{\pi m}{3r}(u+2r)\right]\cos\left[\frac{\pi(n-l)}{9r}(v-w)\right]\\&+\cos\left[\frac{\pi n}{3r}(u+2r)\right]\cos\left[\frac{\pi(l-m)}{9r}(v-w)\right],\end{aligned} \tag{6.15}$$

which never vanishes identically. Figure 6.2 displays the (0,1) symmetric mode.

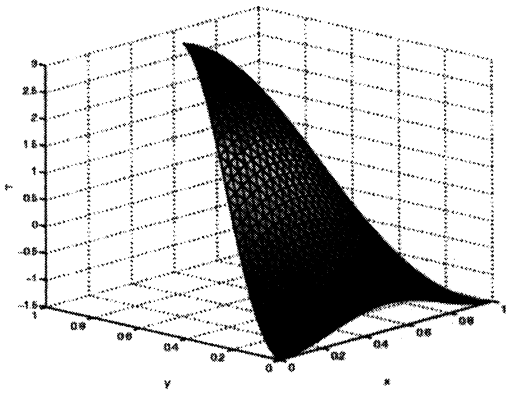

FIGURE 6.2 (0,1) Symmetric mode.

7 CONSTRUCTION OF AN ANTISYMMETRIC MODE

A parallel development is possible for the determination of an antisymmetric mode. In light of the oddness of T_a as a function of $v - w$, we commence with an Ansatz of the form

$$\begin{aligned} T_a = &\cos\left[\frac{\pi l}{3r}(u+2r)\right]\sin[\beta_1(v-w)] \\ &+\cos\left[\frac{\pi m}{3r}(u+2r)\right]\sin[\beta_2(v-w)] \\ &+\cos\left[\frac{\pi n}{3r}(u+2r)\right]\sin[\beta_3(v-w)]. \end{aligned} \tag{7.1}$$

As for the symmetric mode, one can establish that all three terms are in fact necessary for the satisfaction of the Neumann boundary conditions.

Once again we are led to the conditions $l+m+n=0, k^2 = (2/27)(\pi/r)^2[l^2+m^2+n^2] = (4/27)(\pi/r)^2[m^2+mn+n^2]$, and $\beta_1 = \pi(m-n)/(9r), \beta_2 = \pi(n-l)/(9r), \beta_3 = \pi(l-m)/(9r)$. Therefore, we arrive at the antisymmetric mode

$$\begin{aligned} T_a^{m,n} = &\cos\left[\frac{\pi l}{3r}(u+2r)\right]\sin\left[\frac{\pi(m-n)}{9r}(v-w)\right] \\ &+\cos\left[\frac{\pi m}{3r}(u+2r)\right]\sin\left[\frac{\pi(n-l)}{9r}(v-w)\right] \\ &+\cos\left[\frac{\pi n}{3r}(u+2r)\right]\sin\left[\frac{\pi(l-m)}{9r}(v-w)\right], \end{aligned} \tag{7.2}$$

which may be identically zero. Figure 7.1 displays the (0,1) antisymmetric mode.

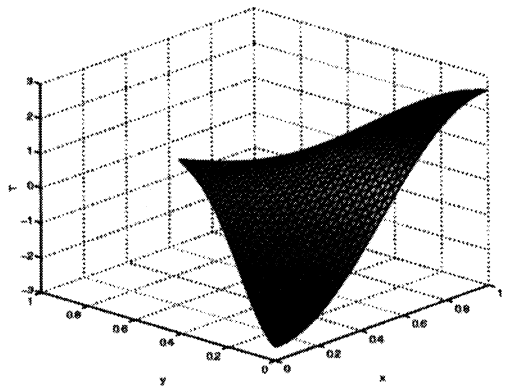

FIGURE 7.1 (0,1) Antisymmetric mode.

8 MODAL PROPERTIES

In what follows, it will be convenient to have the following alternative representations

$$T_s^{m,n} = \frac{1}{2}\left\{\cos\left[\frac{2\pi}{9r}(lu+mv+nw+3lr)\right]+\cos\left[\frac{2\pi}{9r}(nu+mv+lw+3nr)\right]\right.$$
$$+\cos\left[\frac{2\pi}{9r}(mu+nv+lw+3mr)\right]+\cos\left[\frac{2\pi}{9r}(mu+lv+nw+3mr)\right]$$
$$\left.+\cos\left[\frac{2\pi}{9r}(nu+lv+mw+3nr)\right]+\cos\left[\frac{2\pi}{9r}(lu+nv+mw+3lr)\right]\right\}; \tag{8.1}$$

$$T_a^{m,n} = \frac{1}{2}\left\{\sin\left[\frac{2\pi}{9r}(lu+mv+nw+3lr)\right]-\sin\left[\frac{2\pi}{9r}(nu+mv+lw+3nr)\right]\right.$$
$$+\sin\left[\frac{2\pi}{9r}(mu+nv+lw+3mr)\right]-\sin\left[\frac{2\pi}{9r}(mu+lv+nw+3mr)\right]$$
$$\left.+\sin\left[\frac{2\pi}{9r}(nu+lv+mw+3nr)\right]-\sin\left[\frac{2\pi}{9r}(lu+nv+mw+3lr)\right]\right\}, \tag{8.2}$$

obtained from Eqs. (6.15) and (7.2), respectively, by the application of appropriate trigonometric identities.

It is clear from these formulas that both $T_s^{m,n}$ and $T_a^{m,n}$ are invariant under a cyclic permutation of (l, m, n), while $T_s^{n,m} = T_s^{m,n}$ and $T_a^{n,m} = -T_a^{m,n}$ (which are essentially the same since modes are only determined up to a nonzero constant factor). Thus, we need only consider $n \geq m$. Moreover, since $T_{s,a}^{m,n}$, $T_{s,a}^{-n,m+n}$, $T_{s,a}^{-m-n,m}$, $T_{s,a}^{-m,m+n}$, $T_{s,a}^{-m-n,n}$ and $T_{s,a}^{-n,-m}$ all produce equivalent modes, we may also neglect negative m and n.

We may pare this collection further through the following observation due to Lamé [5].

THEOREM 8.1

(i) $T_s^{m,n}$ *never vanishes identically.*
(ii) $T_a^{m,n}$ *vanishes identically if and only if two of* l, m, n *are equal.*

Proof

(i) Note that a symmetric mode is identically zero iff it vanishes along the line of symmetry $v = w$, since the only function both symmetric and antisymmetric is the zero function. Along $v = w$,

$$T_s^{m,n} = \cos\left[\frac{\pi(m+n)}{3r}(u+2r)\right] + \cos\left[\frac{\pi m}{3r}(u+2r)\right] + \cos\left[\frac{\pi n}{3r}(u+2r)\right], \tag{8.3}$$

which may be trigonometrically recast as

$$T_s^{m,n} = 4\cos\left[\frac{\pi(m+n)}{6r}(u+2r)\right]\cos\left[\frac{\pi m}{6r}(u+2r)\right] + \cos\left[\frac{\pi n}{6r}(u+2r)\right] - 1, \tag{8.4}$$

which cannot vanish identically for $-2r \le u \le r$.

(ii) Note that an antisymmetric mode is identically zero iff its normal derivative vanishes along the line of symmetry $v = w$, since the only function both antisymmetric and symmetric is the zero function. Along $v = w$,

$$\begin{aligned}\frac{\partial T_a^{m,n}}{\partial(v-w)} = {} & \frac{\pi(m-n)}{9r}\cos\left[\frac{\pi l}{3r}(u+2r)\right] + \frac{\pi(n-l)}{9r}\cos\left[\frac{\pi m}{3r}(u+2r)\right] \\ & + \frac{\pi(l-m)}{9r}\cos\left[\frac{\pi n}{3r}(u+2r)\right],\end{aligned} \tag{8.5}$$

which may be trigonometrically recast as

$$\begin{aligned}\frac{9r}{\pi}\frac{\partial T_a^{m,n}}{\partial(v-w)} = {} & (m-n)\cos\left[\frac{\pi(m+n)}{3r}(u+2r)\right] \\ & + (m+n)\left\{\cos\left[\frac{\pi m}{3r}(u+2r)\right] - \cos\left[\frac{\pi n}{3r}(u+2r)\right]\right\} \\ & + n\cos\left[\frac{\pi m}{3r}(u+2r)\right] - m\cos\left[\frac{\pi n}{3r}(u+2r)\right].\end{aligned} \tag{8.6}$$

This equals zero iff $m = n$ or $m = -2n$ (*i.e.* $l = n$) or $n = -2m$ (*i.e.* $l = m$). ■

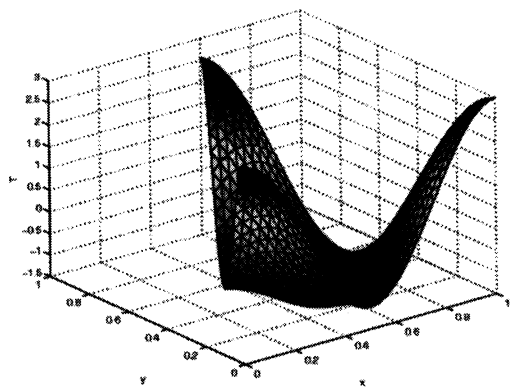

FIGURE 8.1 (1,1) Mode.

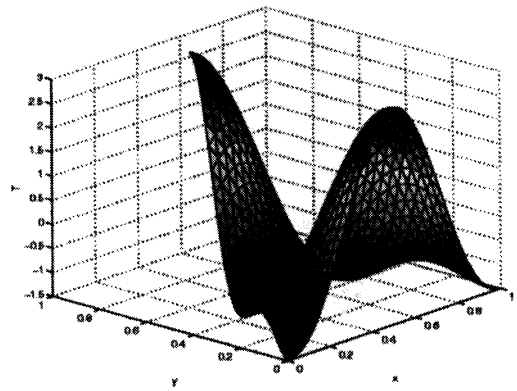

FIGURE 8.2 (0,2) Symmetric mode.

Hence, our system of eigenfunctions is $\{T_s^{m,n}(n \geq m); T_a^{m,n}(n > m)\}$. Figure 8.1 shows the (1,1) mode whereas the symmetric and antisymmetric (0,2) modes are displayed in Figures 8.2 and 8.3 while the symmetric and antisymmetric (1,2) modes are displayed in Figures 8.4 and 8.5, respectively. We next show that this is a complete orthonormal set of eigenfunctions and then go on to explore some features of these modes.

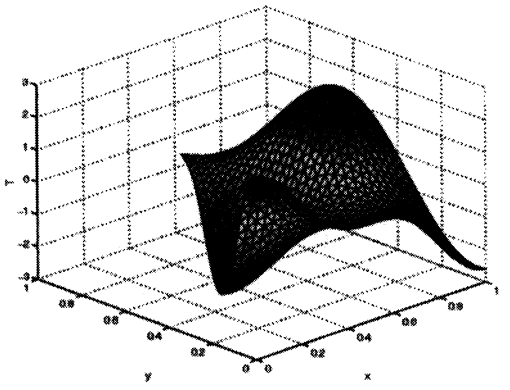

FIGURE 8.3 (0,2) Antisymmetric mode.

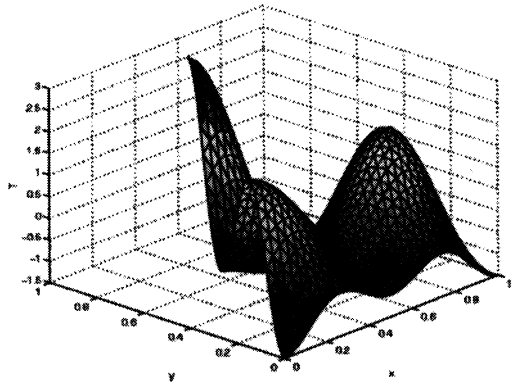

FIGURE 8.4 (1,2) Symmetric mode.

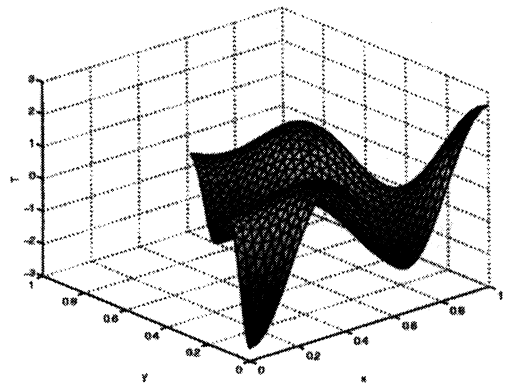

FIGURE 8.5 (1,2) Antisymmetric mode.

8.1 Orthonormality

By Rellich's Theorem [7], eigenfunctions corresponding to distinct eigenvalues are guaranteed to be orthogonal. However, as we shall eventually discover, the multiplicity of the eigenvalues given by Eq. (6.14) is quite a complicated matter. Thus, direct integrations employing Eq. (8.1) and (8.2) confirm the orthogonality of our collection of eigenfunctions $\{T_s^{m,n}(n \geq m); T_a^{m,n}(n > m)\}$.

Furthermore, they may be normalized using

$$\|T_s^{m,n}\|^2 = \frac{9r^2\sqrt{3}}{4} = \|T_a^{m,n}\|^2 \quad (m \neq n), \tag{8.7}$$

$$\|T_s^{m,m}\|^2 = \frac{9r^2\sqrt{3}}{2} \quad (m^2 + n^2 \neq 0), \tag{8.8}$$

and

$$\|T_s^{0,0}\|^2 = 27r^2\sqrt{3}, \tag{8.9}$$

by employing the inner product $\langle f, g\rangle = \int\int_\tau fg \, dA$.

8.2 Completeness

It is not *a priori* certain that the collection of eigenfunctions $\{T_s^{m,n}, T_a^{m,n}\}$ constructed above is complete. For domains which are the Cartesian product of intervals in an orthogonal coordinate system, such as rectangles and annuli, completeness of the eigenfunctions formed from products of one-dimensional counterparts has been established [16]. Since the equilateral triangle is not such a domain, we must employ other devices in order to establish completeness. We follow the lead of Práger [12] and appeal to the well-known completeness of the corresponding eigenfunctions of the rectangle.

For this purpose, we now introduce the triangle-to-rectangle (TTR) transformation pictorialized in Figure 8.6 for symmetric modes and in Figure 8.7 for antisymmetric modes. In these figures, a solid line represents a Dirichlet condition ($T = 0$) and a dashed line a Neumann condition ($\partial T/\partial \nu = 0$), while the patterns of $\pm$ signify symmetry/antisymmetry.

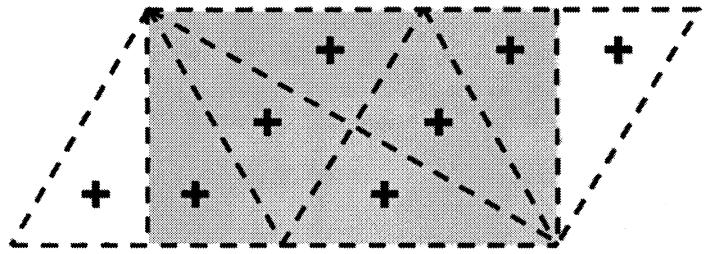

FIGURE 8.6 Triangle-to-rectangle transformation (symmetric mode).

Restricting attention to the right half of the equilateral triangle, this coincides with the prolongation transformation of Práger [12].

Commencing with the equilateral triangle in the southwest corner of each diagram, we construct the remainder of each figure by performing three symmetric reflections across triangle edges as specified by the Fundamental Theorem. In both cases, this leaves us with a (shaded) rectangle of dimensions $3h/2 \times \sqrt{3}h/2$.

For the symmetric mode (Fig. 8.6), this rectangle has strictly Neumann boundary conditions, while, for the antisymmetric mode (Fig. 8.7), there are Neumann boundary conditions along the top and bottom and Dirichlet boundary conditions on the sides. In both cases, the corresponding eigenfunctions of the rectangle are known to be complete. By our construction procedure for the modes of the equilateral triangle, they are seen to be precisely the restriction of the corresponding modes of the associated rectangle possessing the indicated pattern of nodal and antinodal lines.

For example, in order to construct a mode of the rectangle $[\sqrt{3}r, 4\sqrt{3}r] \times [0, 3r]$ of Figure 8.6 with the displayed antinodal lines, we may confine ourselves to making the mode symmetric about the indicated diagonal $y = 4r - x/\sqrt{3}$ since the remaining antinodal lines would then follow immediately from the Fundamental Theorem. We do this by suitably combining the known complete orthogonal rectangular modes of the form $\cos[\mu\pi/(3r)(3r - y)] \cos[\nu 2\pi/(3\sqrt{3}r)(x - 3r)]$, where μ and ν are positive integers.

Although this process is laborious, it is identical to that outlined in Sections 6 and 7 for the construction of T_s and T_a. The end result is that these rectangular modes must be combined in triplets satisfying $\mu_1 + \mu_2 + \mu_3 = 0$, $\nu_1 = \mu_2 - \mu_3$, $\nu_2 = \mu_3 - \mu_1$, $\nu_3 = \mu_1 - \mu_2$. Hence, any such mode of the rectangle will be given by a linear combination of the modes $T_s^{m,n}$ of Eq. (6.15).

Similar considerations applied to the rectangle of Figure 8.7, whose modes are $\cos[\mu\pi/(3r)(3r - y)] \sin[\nu 2\pi/(3\sqrt{3}r)(x - 3r)]$, yield the one-to-one correspondence between $T_a^{m,n}$ of Eq. (7.2) and the modes of this rectangle which vanish along the indicated diagonal.

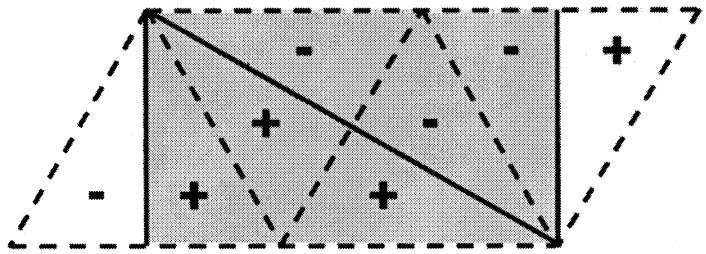

FIGURE 8.7 Triangle-to-rectangle transformation (antisymmetric mode).

Thus, if the equilateral triangle were to possess either a symmetric or an antisymmetric mode not expressible as a linear combination of those we have found above then the same would be true for its extension to the associated rectangle by the TTR transformation. This contradiction establishes that our collection of equilateral triangular modes is indeed complete.

8.3 Nodal/Antinodal Lines

As evidenced by Figure 6.1, the first eigenfunction of an eigenvalue problem can have no nodal lines in the interior of the domain and thus must be of the same sign everywhere [1]. Hence, every other eigenfunction orthogonal to it must have nodal lines.

The structure of the nodal lines is nontrivial. For example, based upon the picture of the (1,1) mode displayed in Figure 8.1, one might posit that the line segments connecting the midpoints of the triangle sides are nodal lines. However, this cannot be the case since it clearly does not possess the antisymmetry required by the Fundamental Theorem. We next consider some properties of nodal/antinodal lines.

We commence by reconsidering the case $m = n$. Recall that we have already determined that $T_a^{m,m} \equiv 0$. Furthermore, in this case, we may combine the terms of Eq. (8.1) to yield

$$T_s^{m,m} = \cos\left[\frac{2\pi m}{3r}(r-u)\right] + \cos\left[\frac{2\pi m}{3r}(r-v)\right] + \cos\left[\frac{2\pi m}{3r}(r-w)\right], \tag{8.10}$$

which clearly illustrates that any permutation of (u, v, w) leaves $T_s^{m,m}$ invariant. This is manifested geometrically in the invariance of $T_s^{m,m}$ under a 120° rotation about the triangle center (see Fig. 8.8). This invariance will henceforth be termed rotational symmetry.

We next rewrite Eq. (8.10) as

$$T_s^{m,m} = (-1)^m 4\cos\left[\frac{\pi m}{3r}(r-u)\right]\cos\left[\frac{\pi m}{3r}(r-v)\right]\cos\left[\frac{\pi m}{3r}(r-w)\right] - 1. \tag{8.11}$$

Thus, the nodal lines even in this special case are given by the transcendental equation obtained by setting this expression to zero.

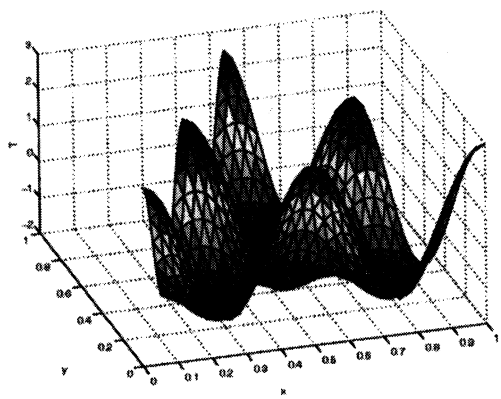

FIGURE 8.8 (2,2) Mode.

In spite of this, there is in fact an inherent structure to the antinodal lines when $m = n$. Straightforward differentiation of Eq.(8.10) establishes that $\partial T_s^{m,m}/\partial u\big|_{v=r-(k/m)3r\ (k=0,\ldots,m)} = 0$. Thus, by invoking rotational symmetry, an antinodal line ($\partial T_s^{m,m}/\partial v = 0$) occurs at

$$u = r - \frac{k}{m}3r; \quad v = r - \frac{k}{m}3r; \quad w = r - \frac{k}{m}3r \ (k = 0, \ldots, m). \tag{8.12}$$

That is, there is a network of $m - 1$ equidistant antinodal lines parallel to each side of the triangle which subdivides it into m^2 congruent equilateral triangles, each supporting a portion of the mode similar to the (1,1) mode and "in-phase" with one another. This is in evidence in Figure 8.8.

As first pointed out by Lamé [5], the modes $T_s^{m,m}$ are not the only ones that are rotationally symmetric.

THEOREM 8.2

(i) *$T_s^{m,n}$ is rotationally symmetric if and only if $m \equiv n(\equiv l)$* (mod 3).
(ii) *$T_a^{m,n}$ is rotationally symmetric if and only if $m \equiv n(\equiv l)$* (mod 3).

Proof

(i) $T_s^{m,n}$ is rotationally symmetric iff it is symmetric about the line $v = u$. This can occur if the normal derivative, $\partial T^{m,n}/\partial v$ vanishes there. Thus, we require that

$$\begin{aligned}\frac{\partial T_s^{m,n}}{\partial(v-u)}\Big|_{v=u} = -\frac{1}{2}\Bigg\{&(m-l)\sin\left[\frac{2\pi}{9r}(lu+mu-2nu+3lr)\right]\\ &+(m-n)\sin\left[\frac{2\pi}{9r}(nu+mu-2lu+3nr)\right]\\ &+(n-m)\sin\left[\frac{2\pi}{9r}(mu+nu-2lu+3mr)\right]\\ &+(l-m)\sin\left[\frac{2\pi}{9r}(mu+lu-2nu+3mr)\right]\\ &+(l-n)\sin\left[\frac{2\pi}{9r}(nu+lu-2mu+3nr)\right]\\ &+(n-l)\sin\left[\frac{2\pi}{9r}(lu+nu-2mu+3lr)\right]\Bigg\} = 0,\end{aligned} \tag{8.13}$$

derived from Eq. (8.1). These terms cancel pairwise iff $m \equiv n(\equiv l)$ (mod3).
(ii) $T_a^{m,n}$ is rotationally symmetric if it is antisymmetric about the line $v = u$.

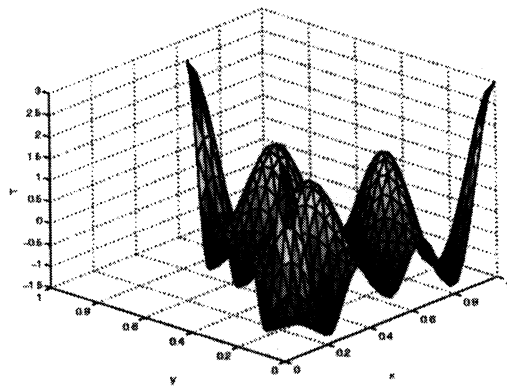

FIGURE 8.9 (1,4) Symmetric mode.

This can occur iff $T_a^{m,n}$ vanishes there. Thus, we require that

$$\begin{aligned} T_a^{m,n}|_{v=u} = \frac{1}{2}\Bigg\{ & \sin\left[\frac{2\pi}{9r}(lu + mu - 2nu + 3lr)\right] \\ & - \sin\left[\frac{2\pi}{9r}(nu + mu - 2lu + 3nr)\right] \\ & + \sin\left[\frac{2\pi}{9r}(mu + nu - 2lu + 3mr)\right] \\ & - \sin\left[\frac{2\pi}{9r}(mu + lu - 2nu + 3mr)\right] \\ & + \sin\left[\frac{2\pi}{9r}(nu + lu - 2mu + 3nr)\right] \\ & - \sin\left[\frac{2\pi}{9r}(lu + nu - 2mu + 3lr)\right]\Bigg\} = 0, \end{aligned} \tag{8.14}$$

derived from Eq. (8.2). These terms cancel pairwise iff $m \equiv n(\equiv l)$ (mod3). ■

This is illustrated in Figures 8.9 and 8.10 which display the symmetric and antisymmetric (1,4) modes, respectively.

Finally, we offer the following new result.

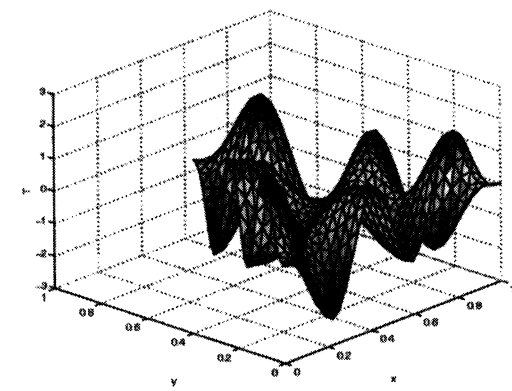

FIGURE 8.10 (1,4) Antisymmetric mode.

THEOREM 8.3 *The volume under $T_s^{m,n}$ is equal to zero if and only if $m^2 + n^2 \neq 0$.*

Proof The volume under $T_s^{0,0}$ is obviously nonzero. Also, by Rellich's Theorem [7], eigenfunctions corresponding to distinct eigenvalues are orthogonal. Hence, all of the other modes $T_s^{m,n}(m^2 + n^2 \neq 0)$ are orthogonal to $T_s^{0,0} = 3$ and thus the volume under these modes is equal to zero. ■

9 SPECTRAL PROPERTIES

In those physical problems in which Eq. (2.1) arises, the frequency $f_{m,n}$ is proportional to the square root of the eigenvalue. Hence, from Eq. (6.14), we arrive at

$$f_{m,n} \propto \frac{4\pi}{3h}\sqrt{\ell}; \quad \ell := m^2 + mn + n^2. \tag{9.1}$$

Thus, the spectral structure of the equilateral triangle hinges upon the number theoretic properties of the binary quadratic form $m^2 + mn + n^2$.

Since $T_s^{m,n}$ and $T_a^{m,n}$ both correspond to the same frequency $f_{m,n}$ given by Eq. (9.1), it follows that all eigenvalues corresponding to $m \neq n$ have multiplicity equal to at least two. However, this model degeneracy, as it is known in the engineering literature, extends also to the case $m = n$. For example, the (7,7) and (2,11) modes, both corresponding to $\ell = 147$, share the same frequency. In fact, the multiplicity question is quite deep and we defer to [9] for its definitive treatment.

Turning to the specific application of the vibrating equilateral triangular membrane for the sake of definiteness, the collection of frequencies $\{f_{m,n}\}$ possesses an inherent structure. Specifically, we can partition this collection of frequencies into distinct "harmonic sequences" so that, within such a sequence, all frequencies are integer multiples of a "fundamental frequency". Complete details appear in [9].

10 NEUMANN FUNCTION

Using Eqs. (6.15), (7.2), and (8.7)–(8.9), we may define the orthonormal system of eigenfunctions

$$\phi_s^{m,n} = \frac{T_s^{m,n}}{\|T_s^{m,n}\|} \quad (m = 0, 1, 2, \ldots; n = m, \ldots), \tag{10.1}$$

$$\phi_a^{m,n} = \frac{T_a^{m,n}}{\|T_a^{m,n}\|} \quad (m = 0, 1, 2, \ldots; n = m + 1, \ldots), \tag{10.2}$$

together with their corresponding eigenvalues

$$\lambda_{m,n} = \frac{4\pi^2}{27r^2}(m^2 + mn + n^2) \quad (m = 0, 1, 2, \ldots; n = m, \ldots). \tag{10.3}$$

The Neumann function [14] (variously called the modified, generalized, or pseudo Green's function) for the Laplacian with Neumann boundary conditions on an equilateral triangle is then constructed as

$$G(x,y;x',y') = \sum_{m=1}^{\infty} \frac{\phi_s^{m,m}(x,y)\phi_s^{m,m}(x',y')}{\lambda_{m,m}} + \sum_{m=0}^{\infty}\sum_{n=m+1}^{\infty} \frac{\phi_s^{m,n}(x,y)\phi_s^{m,n}(x',y') + \phi_a^{m,n}(x,y)\phi_a^{m,n}(x',y')}{\lambda_{m,n}}. \tag{10.4}$$

This may be employed in the usual fashion to solve the corresponding nonhomogeneous boundary value problem, assuming that it is consistent.

11 RELATED STRUCTURES

We now turn to structures related to the equilateral triangle in the sense that they share some or all of their eigenfunctions. Of particular interest are symmetry/asymmetry considerations which show that the eigenfunctions of the equilateral triangle under mixed boundary conditions (*i.e.* part Dirichlet and part Neumann) are not trigonometric.

11.1 Hemi-Equilateral Triangle

The right triangle obtained by subdividing the equilateral triangle along an altitude is shown in Figure 11.1 and is christened forthwith the **hemi-equilateral triangle**. Thus, it may be characterized as a right triangle whose hypotenuse has precisely twice the length of one of its legs. Following Lamé [5] it is immediate that all of its modes (under Neumann boundary conditions) are obtained by simply restricting the symmetric modes of the equilateral triangle (thereby having an antinodal line along said altitude) to this domain. Rather than subdividing the equilateral triangle to obtain a related structure we may instead consider regions obtainable by combining equilateral triangles. We next consider a couple of examples of this procedure.

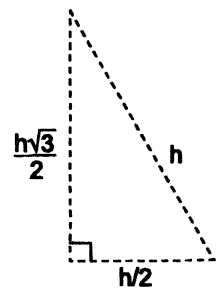

FIGURE 11.1 Hemi-equilateral triangle.

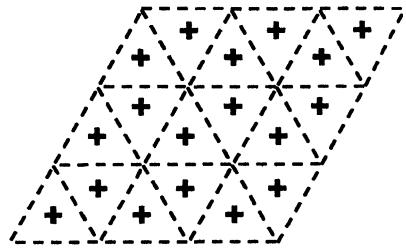

FIGURE 11.2 Symmetric mode of regular rhombus.

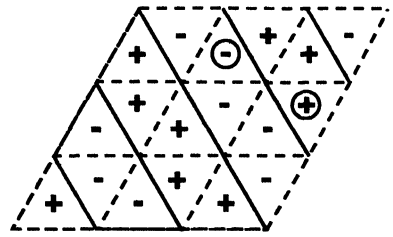

FIGURE 11.3 Antisymmetric mode of regular rhombus.

11.2 Regular Rhombus

Lacking a better term, we will denote a rhombus composed of two equilateral triangles by **regular rhombus**. Thus, a regular rhombus has supplementary angles of 60° and 120°. Any mode of the regular rhombus may be decomposed into the sum of a mode symmetric and a mode antisymmetric about the shorter diagonal. As shown in Figure 11.2 and first observed by Pockels [11], the symmetric modes may all be constructed by symmetric reflection of the modes of the equilateral triangle. However, as shown by Figure 11.3, the antisymmetric modes cannot be so constructed by reflections since this always leads to sign conflicts such as that circled (different signs appearing in positions symmetric about a Neumann line and hence positions of symmetry). A close inspection of Figure 11.3 reveals the following new underlying principle: *The eigenfunctions of the equilateral triangle with two Neumann boundary conditions and one Dirichlet boundary condition are not trigonometric.*

11.3 Regular Hexagon

A similar situation obtains for a regular hexagon which, of course, can be decomposed into six equilateral triangles. As shown in Figure 11.4 and first observed by Pockels [11], any fully symmetric mode (*i.e.* one where all of the edges of the component equilateral triangles are antinodal lines) can be constructed by symmetric reflection of the modes of the equilateral triangle. Yet, any fully antisymmetric mode, which is composed of antisymmetric reflections about the interior triangle edges cannot be so constructed due to the inevitable sign conflicts shown circled. A careful perusal of Figure 11.5 reveals the following new underlying principle: *The eigenfunctions of the equilateral triangle with two Dirichlet boundary conditions and one Neumann boundary condition are not trigonometric.*

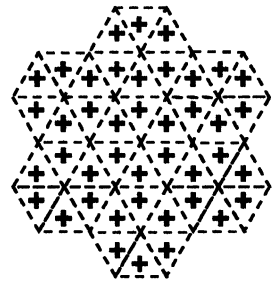

FIGURE 11.4 Fully symmetric mode of regular hexagon.

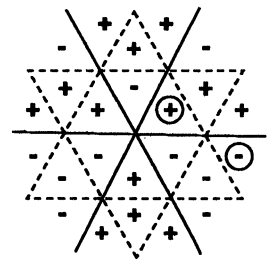

FIGURE 11.5 Fully antisymmetric mode of regular hexagon.

12 CONCLUSION

In the foregoing, we have filled a prominent gap in the applied mathematical literature by providing a complete, direct, and elementary derivation of Lamé's formulas for the eigenfunctions of the equilateral triangle under Neumann boundary conditions. In addition to its innate mathematical interest, this problem is of practical interest as it relates to the calibration of numerical algorithms for approximating the eigenvalues of the Laplacian upon triangulated domains.

In addition, we have established the orthonormality and completeness of this collection of eigenfunctions using the simplest of mathematical tools. Furthermore, we have made an extensive investigation of the properties, especially of the nodal/antinodal lines, of these modes. Lastly, the Neumann function has been specified and related structures have been considered. Part I of this work [8] presented a parallel treatment of the Dirichlet problem while Part III will deal with the much more difficult Robin problem.

Acknowledgement

The author thanks Mrs. Barbara A. McCartin for her indispensable aid in constructing the figures.

References

[1] Courant, R. and Hilbert, D. (1953) *Methods of Mathematical Physics* (Vol. I). New York, NY: Wiley-Interscience, p. 451.

[2] Gray, J. (1993) Möbius's Geometrical Mechanics. In: Fauvel, J., *et al.* (Eds.), *Möbius and His Band.* New York, NY: Oxford.

[3] Jones, D. S. (1986) *Acoustic and Electromagnetic Waves.* Clarendon, Oxford.

[4] Lamé, G. (1833) Mémoire sur la propagation de la chaleur dans les polyèdres, *Journal de l'École Polytechnique*, **22**, 194–251.
[5] —, (1861) *Leçons sur la Théorie Analytique de la Chaleur.* Paris: Mallet-Bachelier.
[6] —, (1866) *Leçons sur la Théorie Mathématique de l'Élasticité des Corps Solides* (Deuxième Èdition). Paris: Gauthier-Villars.
[7] MacCluer, C. R. (1994) *Boundary Value Problems and Orthogonal Expansions: Physical Problems from a Sobolev Viewpoint.* New York, NY: IEEE Press.
[8] McCartin, B. J. (2002) Eigenstructure of the equilateral triangle, Part I: The Dirichlet problem, *SIAM Review*, to appear.
[9] McCartin, B. J. (2002) Modal degeneracy in equilateral triangular waveguides, *J. Electromagn. Waves and Applic.*, **16**(7), 943–956.
[10] Pinsky, M. A. (1980) The eigenvalues of an equilateral triangle, *SIAM J. Math. Anal.*, **11**(5), 819–827.
[11] Pockels, F. (1891) *Über die partielle Differentialgleichung* $\Delta u + k^2 u = 0$. Leipzig: Teubner.
[12] Práger, M. (1998) Eigenvalues and eigenfunctions of the Laplace operator on an equilateral triangle, *Applic. Math.*, **43**(4), 311–320.
[13] Rayleigh, L. (1894) *The Theory of Sound* (2nd ed.). Mineola, NY: Dover, p. 318.
[14] Roach, G. F. (1982) *Green's Functions* (2nd ed.). London: Cambridge.
[15] Schelkunoff, S. A. (1943) *Electromagnetic Waves.* Princeton, NJ: Van Nostrand, pp. 393–396.
[16] Strauss, W. A. (1992) *Partial Differential Equations: An Introduction.* New York, NY: Wiley.

Mathematical Problems in Engineering

Special Issue on
Modeling Experimental Nonlinear Dynamics and Chaotic Scenarios

Call for Papers

Thinking about nonlinearity in engineering areas, up to the 70s, was focused on intentionally built nonlinear parts in order to improve the operational characteristics of a device or system. Keying, saturation, hysteretic phenomena, and dead zones were added to existing devices increasing their behavior diversity and precision. In this context, an intrinsic nonlinearity was treated just as a linear approximation, around equilibrium points.

Inspired on the rediscovering of the richness of nonlinear and chaotic phenomena, engineers started using analytical tools from "Qualitative Theory of Differential Equations," allowing more precise analysis and synthesis, in order to produce new vital products and services. Bifurcation theory, dynamical systems and chaos started to be part of the mandatory set of tools for design engineers.

This proposed special edition of the *Mathematical Problems in Engineering* aims to provide a picture of the importance of the bifurcation theory, relating it with nonlinear and chaotic dynamics for natural and engineered systems. Ideas of how this dynamics can be captured through precisely tailored real and numerical experiments and understanding by the combination of specific tools that associate dynamical system theory and geometric tools in a very clever, sophisticated, and at the same time simple and unique analytical environment are the subject of this issue, allowing new methods to design high-precision devices and equipment.

Authors should follow the Mathematical Problems in Engineering manuscript format described at http://www.hindawi.com/journals/mpe/. Prospective authors should submit an electronic copy of their complete manuscript through the journal Manuscript Tracking System at http://mts.hindawi.com/ according to the following timetable:

Manuscript Due	February 1, 2009
First Round of Reviews	May 1, 2009
Publication Date	August 1, 2009

Guest Editors

José Roberto Castilho Piqueira, Telecommunication and Control Engineering Department, Polytechnic School, The University of São Paulo, 05508-970 São Paulo, Brazil; piqueira@lac.usp.br

Elbert E. Neher Macau, Laboratório Associado de Matemática Aplicada e Computação (LAC), Instituto Nacional de Pesquisas Espaciais (INPE), São Josè dos Campos, 12227-010 São Paulo, Brazil ; elbert@lac.inpe.br

Celso Grebogi, Department of Physics, King's College, University of Aberdeen, Aberdeen AB24 3UE, UK; grebogi@abdn.ac.uk